Intracellular photodynamic therapy with photosensitizer-nanoparticle conjugates: cancer therapy using a 'Trojan horse'

Martina E. Wieder,[a] Duncan C. Hone,[a] Michael J. Cook,[a] Madeleine M. Handsley,[b] Jelena Gavrilovic[b] and David A. Russell*[a]

Received 24th February 2006, Accepted 24th May 2006
First published as an Advance Article on the web 21st June 2006
DOI: 10.1039/b602830f

Phthalocyanine-nanoparticle conjugates have been designed and synthesised for the delivery of hydrophobic photosensitizers for photodynamic therapy (PDT) of cancer. The phthalocyanine photosensitizer stabilized gold nanoparticles have an average diameter of 2–4 nm. The synthetic strategy interdigitates a phase transfer reagent between phthalocyanine molecules on the particle surface that solubilises the hydrophobic photosensitizer in polar solvents enabling delivery of the nanoparticle conjugates to cells. The phthalocyanine is present in the monomeric form on the nanoparticle surface, absorbs radiation maximally at 695 nm and catalytically produces the cytotoxic species singlet oxygen with high efficiency. These properties suggest that the phthalocyanine-nanoparticle conjugates are ideally suited for PDT. In a process that can be considered as cancer therapy using a 'Trojan horse', when the nanoparticle conjugates are incubated with HeLa cells (a cervical cancer cell line), they are taken up thus delivering the phthalocyanine photosensitizer directly into the cell interior. Irradiation of the nanoparticle conjugates within the HeLa cells induced substantial cell mortality through the photodynamic production of singlet oxygen. The PDT efficiency of the nanoparticle conjugates, determined using colorimetric assay, was twice that obtained using the free phthalocyanine derivative. Following PDT with the nanoparticle conjugates, morphological changes to the HeLa cellular structure were indicative of cell mortality *via* apoptosis. Further evidence of apoptosis was provided through the bioluminescent assay detection of caspase 3/7. Our results suggest that gold nanoparticle conjugates are an excellent vehicle for the delivery of surface bound hydrophobic photosensitizers for efficacious photodynamic therapy of cultured tumour cells.

Introduction

An area of research where it is thought that nanotechnology will have a profound impact is within medical science. There is considerable worldwide research effort in developing nanoscale systems, particularly for use in cancer imaging and therapy. Two notable examples of nanoscale systems developed to date are: semi-conductor quantum dots for use in both *in vivo* targeting and imaging of human prostate cancer grown in mice;[1] and silica core-gold shell nanoparticles which have been used both to photothermally induce *in vitro* mortality of human breast carcinoma cells[2] and subsequently for the *in vivo* destruction of murine colon carcinoma cells grown in an animal model.[3]

We are interested in developing a drug delivery system based on nanoparticle technology for the photodynamic therapy (PDT) of cancer indications. PDT is a cancer treatment modality which combines the use of a photoactive drug, termed a photosensitizer, with light to cause selective damage of the target tissue. Visible light is used to stimulate the photosensitizer into an electronically excited state. The excited state energy is transferred to ground state molecular oxygen to produce an excited species known as singlet oxygen. Singlet oxygen is a highly oxidising form of oxygen and is cytotoxic. It is the cytotoxicity of singlet oxygen which is key to PDT as a cancer treatment.

While the clinical potential of PDT has been recognized for over 25 years, approval of a photosensitizer for oncological indications was first granted in 1995. The first approved photosensitizer was hematoporphyrin derivative (Photofrin) and subsequently 3 other drugs have received regulatory approval, *viz.*: meta-tetrahydroxyphenyl chlorin (Foscan); 5-aminolevulinic acid (Levulan) and methyl 5-aminolevulinate (Metvix). The latter two drugs are not photosensitizers but are converted by the body to protoporphyrin IX (or the methyl derivative for Metvix) *via* the heme biosynthetic pathway. Protoporphyrin IX is a photosensitizer and consequently produces singlet oxygen when stimulated by light. The current status of PDT in cancer treatment has been recently reviewed by Brown *et al.*[4]

While excellent clinical results are obtained with the current photosensitizers a number of improvements are sought which would enhance the efficiency of PDT treatment. These improvements include: isomerically pure photosensitizers; photosensitizers which absorb light in the far-red region of the electromagnetic spectrum, as human tissue transmits these wavelengths preferentially thus enabling access to deeper residing tumours;[4] enhanced efficiency of singlet oxygen production, thereby reducing the concentration of the photosensitizer necessary to treat the tumour; and increased selectivity of biodistribution of the photosensitizer

[a]*School of Chemical Sciences and Pharmacy, University of East Anglia, Norwich, UK NR4 7TJ. E-mail: d.russell@uea.ac.uk*
[b]*School of Biological Sciences, University of East Anglia, Norwich, UK NR4 7TJ*

in the tumour tissue, this latter improvement is particularly important as skin photosensitivity is known to be a key limitation currently.

Phthalocyanines are a class of compounds which have been shown to successfully address all of these issues.[5] However, the parent phthalocyanine molecule is hydrophobic and needs to be incorporated within a liposomal formulation, for example, for successful delivery. Water soluble phthalocyanines can be made and indeed disulfonated aluminium phthalocyanine has received approval for use in Russia.[4] However, hydrophobic photosensitizers have been shown to exhibit substantially greater PDT performance[6,7]—the obvious drawback being the need for lipid-based delivery systems in order to target the tumour tissue with such photosensitizers. We have been studying a series of zinc phthalocyanine derivatives for PDT which possess eight substituents surrounding the parent macrocyclic ring structure.[5] We have shown that these photosensitizer molecules exhibit excellent PDT action,[8,9] although a Cremophor emulsion was required in order to facilitate delivery into the animal model.

In order to avoid the use of such emulsions we have recently developed a nanoparticle approach for photosensitizer drug delivery.[10] Our delivery system is based on gold nanoparticles whereby the photosensitizer is bound to the surface of the nanoparticle. The surface bound photosensitizer exhibits a remarkable enhancement of the singlet oxygen quantum yield ($\Phi_\Delta = 0.65$) as compared with the free photosensitiser ($\Phi_\Delta = 0.45$). It is thought that this 50% enhancement in Φ_Δ is due to the presence of an associated phase transfer agent (tetraoctylammonium bromide; TOAB) which increases the triplet energy transfer to molecular oxygen. Subsequently, Prasad *et al.* have reported a silica nanoparticle based delivery approach whereby the photosensitizer was encapsulated within the nanoparticles achieving excellent cell kill results with their *in vitro* study.[11] Other nanoscale systems that have been proposed for application in PDT include semiconductor quantum dots,[12,13] polymeric nanoparticles for the encapsulation of photosensitizers[14,15] and most recently, iron oxide nanoparticles for combined hyperthermia and photodynamic therapies.[16] In a recent review where the silica and gold nanoparticle systems were compared as photosensitizer delivery vehicles,[17] it was speculated that the surface bound photosensitizer (on the gold nanoparticle) may present an advantage over an encapsulated photosensitizer in that the generated singlet oxygen would not need to diffuse out of the porous particle structure to elicit cell kill. This present paper reports on a cellular study (with HeLa cells, a well established tumour cell line originating from a cervical epithelial tumour) using our photosensitizer-nanoparticle conjugates for photodynamic therapy.

In order to exemplify our gold nanoparticle delivery technology we chose to use a phthalocyanine derivative with consideration of the improved PDT performance of this class of molecules, although other photosensitizers could be readily delivered using this approach. To attach the phthalocyanine molecule to the gold surface, the photosensitizer has been derivatized with a thiol moiety. The thiol provides a direct linkage to the gold nanoparticle surface *via* self-assembly. The photosensitizer stabilized gold nanoparticles are formulated using a gold salt, a phase transfer reagent (TOAB), the thiolated phthalocyanine derivative and sodium borohydride as a reductant. The resulting product is designed to provide a 3-component system containing the photosensitizer and phase transfer reagent bound to the surface of the gold nanoparticles. Importantly, while the free phthalocyanine derivative is only soluble in organic solvents, such as toluene, the presence of the phase transfer reagent facilitates solubilisation of the photosensitizer-nanoparticle conjugates in polar solvents such as ethanol. Such solubility and the overall size of the phthalocyanine-nanoparticle conjugates are essential design features as they enable the delivery and the subsequent internalisation of the conjugates by the cells. Irradiation of the internalised phthalocyanine-nanoparticle conjugates induces mortality of the cancerous cells—a process which we consider as cancer therapy using a 'Trojan horse'.

Experimental

Materials

All reagents were purchased from Sigma-Aldrich, unless otherwise stated, were of analytical reagent grade or better and used as received. Millipore® water (resistivity $\geq$18 MΩ cm) was used throughout.

Synthesis and characterization of 1,4,8,11,15,18-hexahexyl-22-methyl-25-(11-mercaptoundecyl) phthalocyaninato zinc (1) stabilized gold nanoparticles. A communication of the synthesis of the photosensitizer stabilized nanoparticles has been made previously.[10] $HAuCl_4$ (3.6 mg) was dissolved in water (7 mL) to give a clear yellow solution. Tetraoctylammonium bromide (TOAB) (21.2 mg) was dissolved in toluene (20 mL). The two solutions were mixed to give a dark red solution. The solution was stirred for 20 min, after which time the aqueous phase became colourless and was removed. The zinc phthalocyanine derivative (**1**) (12.5 mg) was added to the toluene layer and stirred for 10 min. A freshly prepared solution of sodium borohydride ($NaBH_4$) reductant (4.4 mg in 7 mL water) was rapidly added and the solution vigorously stirred for 3 h. Separation of free and nanoparticle bound phthalocyanine was achieved using preparative silica thin layer chromatography (TLC) in a solvent of toluene: methanol (95 : 5). Two bands were obtained. The top band (free phthalocyanine) was dissolved in toluene while the bottom stop (phthalocyanine-nanoparticle conjugate) was dissolved in ethanol. The phthalocyanine-nanoparticle conjugates are soluble in ethanol due to the interdigitation of TOAB with the self-assembled phthalocyanine derivatives.[10] A total volume of 150 mL of ethanol was used as three TLC plates, used for the separation of free and bound phthalocyanine, were combined. Each fraction was filtered and the phthalocyanine-nanoparticle conjugate solution was concentrated by rotary evaporation (Buchi Rotavapor R-200, UK) to approximately 40 mL. Concentration values quoted for the phthalocyanine-nanoparticle conjugates refer to the concentration of the phthalocyanine derivative assembled on the gold surface as determined by fluorescence spectroscopy using a standard calibration curve.

UV-visible and fluorescence spectroscopy of the phthalocyanine-nanoparticle conjugates were performed using a Hitachi U-3000 UV-visible and a FluoroMax-2 (ISA Instruments S.A.) fluorescence spectrometer respectively. Both showed the presence of the phthalocyanine molecule with the characteristic absorbance (λ_{max} = 695 nm) and fluorescence (λ_{em} = 715 nm) maxima of the octyl substituted phthalocyanine

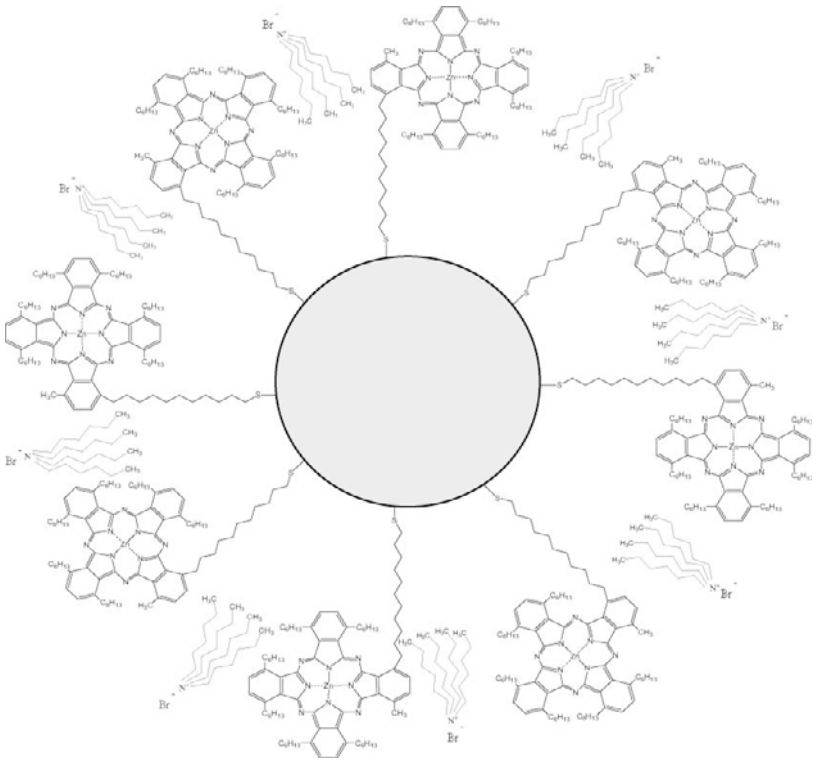

Fig. 1 Schematic representation of the three-component phthalocyanine-nanoparticle conjugates.

derivative.[5,8] Transmission electron microscopy (TEM) (Jeol 2000EX operating at 100 kV) confirmed that the photosensitizer stabilized nanoparticles were 2–4 nm in diameter. Energy dispersive X-ray analysis (EDXA) confirmed the presence of both the phthalocyanine photosensitizer and the TOAB phase transfer reagent on the gold surface by the appearance of Zn(II) (L_α 8.63 keV) and bromine (K_α 11.90; K_β 13.38 keV) signals in the spectrum respectively.[10] A schematic representation of the 3-component phthalocyanine-nanoparticle conjugates is shown in Fig. 1.

Gold nanoparticles stabilized by *N*,*N*,*N*-trimethyl (11-mercaptoundecyl) ammonium chloride (Au–NMe_3^+) and mannose (Au–mannose). For controls, gold nanoparticles that were stabilized with *N*,*N*,*N*-trimethyl (11-mercaptoundecyl) ammonium chloride[18,19] and the carbohydrate mannose[20] were formulated using respective literature procedures. The nanoparticles produced were *ca.* 11 and 16 nm in diameter respectively, as determined by TEM measurements.

Determination of singlet oxygen production using a molecular probe. The detection of singlet oxygen production through the photobleaching of disodium, 9, 10-anthracenedipropionic acid) (ADPA, Invitrogen) was originally reported by Lindig *et al.*[21] This molecular probe has recently been used to assess the singlet oxygen production from photosensitizers encapsulated in silica[11] and polyacrylamide[14] nanoparticle systems. ADPA (70 μL of 5.5 mM aqueous solution) was added to 3 mL ethanol. Phthalocyanine-nanoparticle conjugates (12 μM; 300 μL) and ethanol (2.7 mL) were combined with the ADPA solution. Three control experiments were prepared. The first control combined ADPA with ethanol. The second control combined phthalocyanine-nanoparticle conjugates with ethanol, while the third control combined Au–NMe_3^+ nanoparticles (12 μM; 300 μL) with ethanol and ADPA. The solutions were irradiated with a 690 nm diode laser (Opnext, HL6738MG) at 1.72 mW cm^{-2} for 150 min. UV-visible absorption spectra between 300–800 nm were recorded so that the decreasing absorbance intensity at 400 nm of the ADPA, as a function of singlet oxygen production, was obtained.

***In vitro* photodynamic therapy experiments with HeLa cells.** HeLa cells (American Type Culture Collection) were routinely cultured in 75 cm^3 tissue culture flasks in Dulbecco's Modified Eagle Medium (DMEM) supplemented with 10% fetal calf serum (FCS), 1% penicillin–streptomycin (P–S) and 1% *L*-glutamine (all purchased from Invitrogen Life Sciences).

Phthalocyanine-nanoparticle conjugates were incubated with the HeLa cells, and the effects with, and without, irradiation from the 690 nm diode laser were assessed in terms of the cell viability/cell death using assays and microscopy.

To assess nanoparticle conjugate uptake by the HeLa cells and cellular morphology post-PDT, confocal laser scanning microscopy was used. HeLa cells (25×10^4 cells) were cultured on 42 mm round coverslips in a Petri dish in 5 mL DMEM and then incubated for 24 h. The cells were incubated with 47 μM phthalocyanine-nanoparticle conjugates in 5 mL DMEM for 6 or 16 h. The medium was then changed to phenol red free, air-buffered, L15 medium containing the FCS, P–S and *L*-glutamine supplements and the cells were mounted on a 37 °C heated stage. The cells were observed with a confocal laser scanning microscope (Carl Zeiss, LSM 510 meta) using 633 nm laser excitation with fluorescence emission measurement between 650–720 nm. A 63×, 1.4 NA objective was used to obtain high-resolution images. Differential Interference Contrast (DIC) images were collected

simultaneously with transmitted light from the 633 nm excitation. Images were processed and composite merges were obtained using Adobe Photoshop.

To determine cell viability the colorimetric MTT metabolic activity assay developed by Mossman,[22] and subsequently modified by Prasad and co-workers to incorporate a cell irradiation protocol,[11] was used. HeLa cells (1×10^4 cells well^{-1}) were added to wells of a 96 well microtiter plate (Nunc) with 200 μL DMEM and incubated for 24 h. Phthalocyanine-nanoparticle conjugates (0.5 μL of varying concentrations in ethanol), with 100 μL DMEM, were added to the wells and the plates were returned to the incubator for 2, 4 or 6 h. After incubation, the wells were rinsed three times with phosphate buffered saline (PBS) to remove the nanoparticle conjugates that had not been internalised by the HeLa cells. DMEM (200 μL) was added to the wells and then each well was irradiated using the 690 nm diode laser for varying time periods. The cells were incubated for a further 18 h. Cell viability was assessed using the MTT (3-[4, 5-dimethylthiazol-2-yl]-2, 5 diphenyltetrazolium bromide; Sigma) assay. MTT was dissolved in PBS (5 mg mL^{-1}), and 12.5 μL was added to each well following the 18 h incubation. The cells were then incubated for a further 4 h. The resultant formazan crystals were dissolved in dimethyl sulfoxide (200 μL) and the absorbance intensity measured at 570 nm. Each variable (concentration of nanoparticle conjugates, incubation time and irradiation time) was assessed through MTT assay in triplicate. To ensure reproducible irradiation of the HeLa cells, the intensity of the laser light source was measured on each occasion using a power meter (Power Max 500AD; Molectron).

Apoptosis is a key mechanism of cell death which can be induced by PDT action. To determine whether the phthalocyanine-nanoparticle conjugates induce apoptosis a bioluminescent assay for activation of caspases-3 and -7 (Caspase-Glo™ 3/7 assay; Promega) was used. HeLa cells (1×10^4 cells well^{-1}) were plated on a white-walled 96 well plate (to remove background fluorescence) with 200 μL DMEM and incubated for 24 h. 0.5 μL of the phthalocyanine-nanoparticle conjugates (0.55 μM in ethanol) with 100 μL DMEM were added to the wells and the plate returned to the incubator for 6 h. After incubation, the cells were rinsed 3 times with PBS to remove non-internalised nanoparticles. DMEM (100 μL) was added to the wells, which were then irradiated with the 690 nm diode laser at 1.84 mW cm^{-2} for 10 min each. The irradiated HeLa cells were incubated for 18 h. Caspase-Glo™ 3/7 buffer and lyophilised Caspase-Glo™ substrate (Promega) were stored in a freezer and equilibrated to room temperature (*ca.* 20 ° C) prior to use. The buffer and substrate solutions were combined. Caspase-Glo™ reagent (100 μL) was added to each well. The contents of the wells were mixed on a plate shaker for 30 s. The 96 well plate was incubated at 20 °C for 3 h. The luminescence of the samples was measured using a Wallac Victor 2, 1420 Multilabel Counter. Each assay measurement was replicated at least 3 times.

Results and discussion

The generation of the cytotoxic singlet oxygen using the photosensitizer-nanoparticle conjugates was monitored colorimetrically using the ADPA probe. The photosensitizer-nanoparticle conjugates were irradiated in the presence of the ADPA, the bleaching of which (through the formation of the endoperoxide), was monitored by UV-visible spectroscopy over

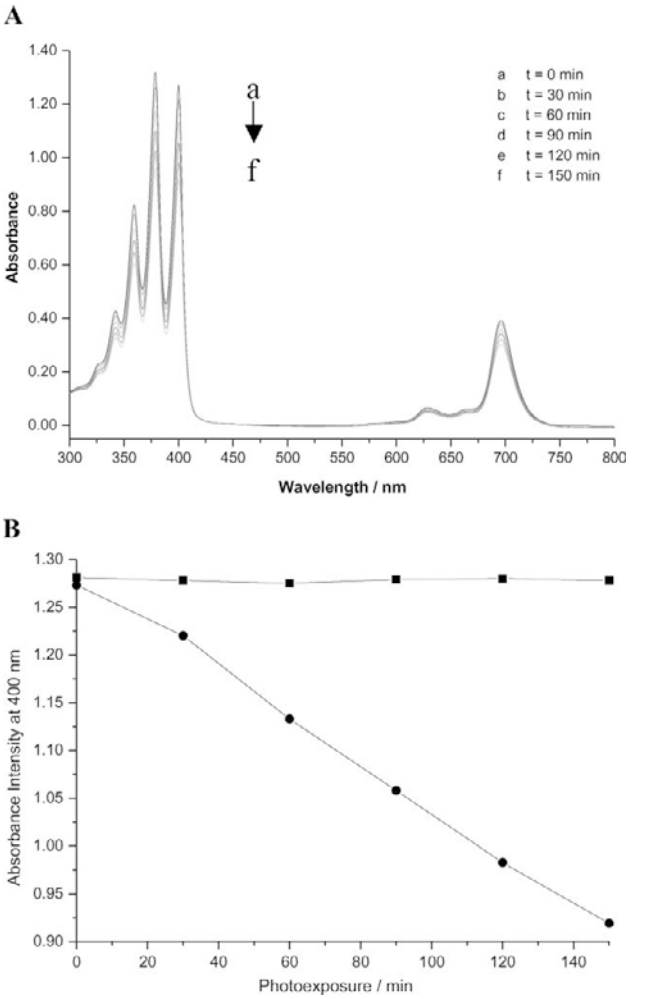

Fig. 2 Variation of the absorption spectrum of ADPA and phthalocyanine-nanoparticle conjugates following irradiation at 690 nm (1.72 mW cm^{-2}). (A) Spectrum showing contributions from both ADPA and phthalocyanine-nanoparticle conjugates. (B) Time-dependent photobleaching of ADPA absorbance as the singlet oxygen, generated by the irradiation (at 690 nm) of phthalocyanine-nanoparticle conjugates (dots), produces the endoperoxide. Au–NMe_3^+ nanoparticles were used as a control (squares).

150 min. The absorption spectrum in Fig. 2(A) shows the presence of both the phthalocyanine assembled on the gold nanoparticles, between 600–750 nm, and the ADPA probe, between 300–425 nm. The spectrum of the nanoparticle conjugates indicates that the phthalocyanine is in the monomeric (non-aggregated) form on the gold nanoparticle surface. This is an important attribute as photosensitizers which aggregate tend to exhibit poor PDT efficacy, invariably due to deactivation of the excited state energy. Following irradiation using the diode laser at 690 nm, the absorbance intensity of the ADPA diminished with time (Fig. 2(A)). The slight decrease of the phthalocyanine absorption bands (Fig. 2(A)) possibly suggests that the generation of the singlet oxygen partially bleaches the nanoparticle conjugates. As a control, Au–NMe_3^+ nanoparticles were also irradiated at 690 nm in the presence of ADPA. The absorbance intensity of ADPA at 400 nm was monitored in the presence of both the phthalocyanine-nanoparticle conjugates and Au–NMe_3^+ nanoparticles in separate

experiments, Fig. 2(B). It is clear that the presence of the photosensitizer on the nanoparticle surface is essential for the production of singlet oxygen as evidenced by the diminution of the absorbance intensity at 400 nm of the ADPA colorimetric probe over the 150 min time interval. This result is in agreement with previous studies where we have detected the evolution of singlet oxygen from such phthalocyanine stabilized nanoparticles using time resolved luminescence measurements, establishing the quantum yield of singlet oxygen production as 0.65.[10] These combined results show that the photosensitizer-nanoparticle conjugates are efficient catalysts for the generation of the cytotoxic singlet oxygen species.

To establish whether photosensitizers can be delivered to cells *via* the nanoparticle vehicle approach, the phthalocyanine-nanoparticle conjugates were incubated with HeLa cells. With consideration of the small size of the nanoparticles it was envisaged that the HeLa cells would internalize the photosensitizer-nanoparticle conjugates through endocytotic processes from the extracellular environment. Indeed internalisation of the photosensitizer-nanoparticle conjugates was readily observed when the particles were incubated with the HeLa cells for 16 h. The uptake of the conjugates by the cells, observed using confocal fluorescence microscopy, is shown in Fig. 3. It can be seen that the nanoparticle conjugates are present throughout the intracellular space, with the exception of the cell nucleus.

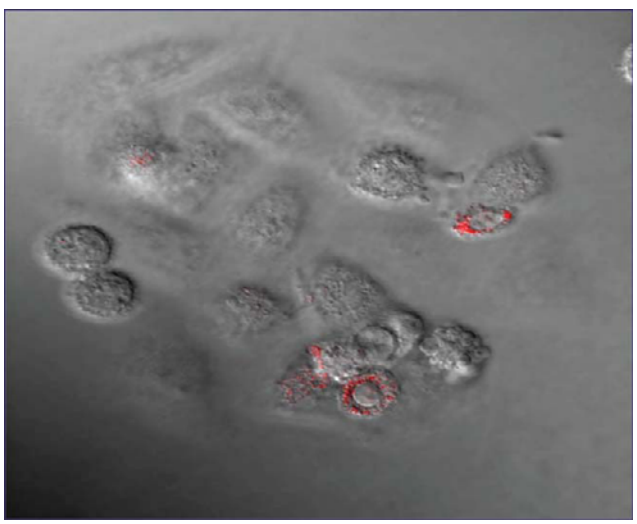

Fig. 3 Combined confocal fluorescence and DIC images of HeLa cells following incubation with phthalocyanine-nanoparticle conjugates. The presence of the nanoparticle conjugates within the HeLa cells can be readily seen from the fluorescence emission (red) following excitation at 633 nm.

To determine the *in vitro* efficiency of the photosensitizer-nanoparticle conjugates for photodynamic therapy, variation and optimization of multiple parameters were required. These parameters included: varying nanoparticle conjugate concentration (0.04–5.42 μM); variation of cell incubation period (2, 4 and 6 h) with the nanoparticle conjugates; and variation of the period of irradiation of the cells (10, 20 and 30 min) using the 690 nm diode laser. Cell assays were used to study each parameter by measurement of cell viability (as % metabolic activity) using the colorimetric MTT reagent. Full controls were undertaken for each variable. The results of these studies are summarised in Fig. 4.

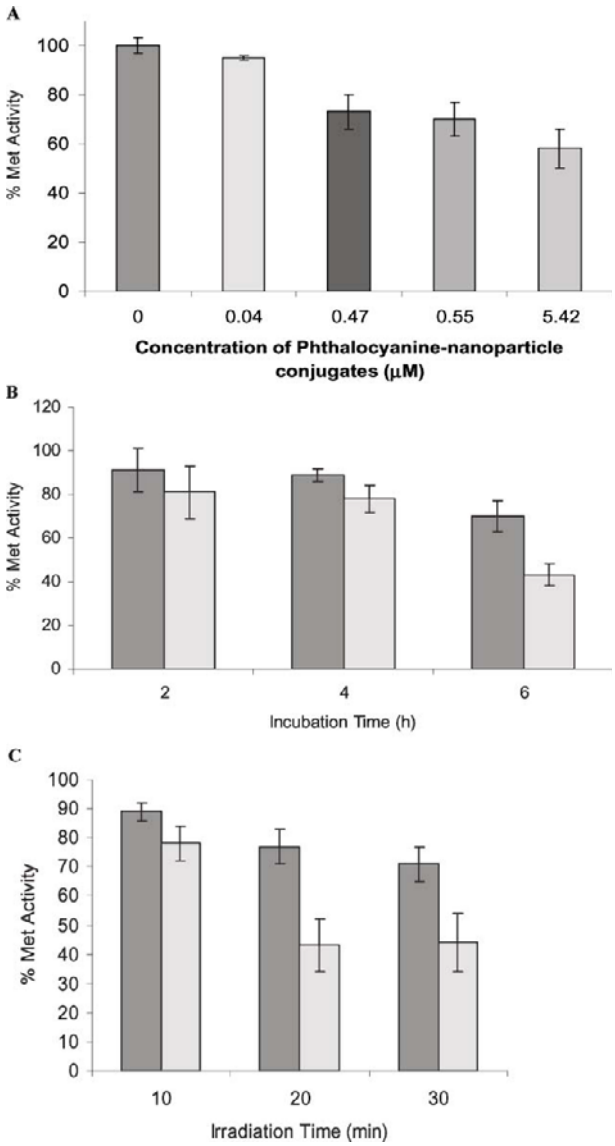

Fig. 4 Variation and optimization of parameters for the *in vitro* PDT of HeLa cells using phthalocyanine-nanoparticle conjugates as determined by MTT assay. All data are an average of 3 replicates for each parameter. (A) Effect of phthalocyanine-nanoparticle conjugate concentration when incubated with the HeLa cells for 6 h. (B) Effect of duration of incubation of 0.55 μM phthalocyanine-nanoparticle conjugates with the HeLa cells for 2, 4 or 6 h before (dark grey) and after (light grey) irradiation with a 690 nm diode laser at 1.84 mW cm^{-1} for 10 min. (C) Effect of duration of irradiation of the 0.55 μM phthalocyanine-nanoparticle conjugates on HeLa cell viability. Cells were irradiated for 10, 20 or 30 min (light grey) (using a 690 nm diode laser at 1.66 mW cm^{-1}). Controls, where the nanoparticle conjugates within the cells were not irradiated are shown for comparison (dark grey).

Fig. 4(A) shows that the HeLa cell viability, as determined by MTT assay, decreases as the concentration of the phthalocyanine-nanoparticles incubated with the cells increases. These dose *versus* metabolic activity data show that the nanoparticle conjugates exhibit a dark-toxicity at higher concentrations when incubated with the cells for 6 h. By decreasing the period of time used to incubate the nanoparticle conjugates (at a concentration of 0.55 μM) from 6 to 4 or 2 h, the dark toxicity effect is reduced

(Fig. 4(B)). Cell survival was *ca.* 90% when a period of either 2 or 4 h was used to incubate the nanoparticle conjugates with the HeLa cells. Cell survival reduced to 70% with a 6 h incubation. When the accumulated nanoparticle conjugates within the cells were irradiated for 10 min using the diode laser at 690 nm, PDT action resulted in a further reduction of the cell viability. With consideration of both the dark toxicity and the PDT effect following irradiation, it was determined that a period of 4 h was the optimal time for the cells to take-up and intracellularly accumulate the nanoparticle conjugates (Fig. 4(B)). The effect of the time of irradiation of the nanoparticle conjugates within the cells (following 4 h incubation) is shown in Fig. 4(C). The data (in Fig. 4(C)) clearly show that the optimum PDT effect is observed when the cells are irradiated for 20 min with the 690 nm light source. From the data shown in Fig. 4, the optimized protocol for the PDT of the cervical cancerous cell line was determined as follows: HeLa cells (1×10^4 cells well^{-1}) were added to the wells of a 96 well plate with 200 μL DMEM and incubated for 24 h. Phthalocyanine-nanoparticle conjugates (0.5 μl of 0.55 μM conjugates in ethanol) with 100 μL DMEM, were added to the wells and the plate was returned to the incubator for 4 h. The wells were rinsed 3 times with PBS to remove non-internalised nanoparticle conjugates. DMEM (200 μL) was added to the wells and then each well was irradiated for 20 min using the 690 nm diode-laser at 1.84 mW cm^{-2}. The HeLa cells were incubated for a further 18 h. The cell viability results, as determined by MTT assay, using this optimised protocol are shown in Fig. 5.

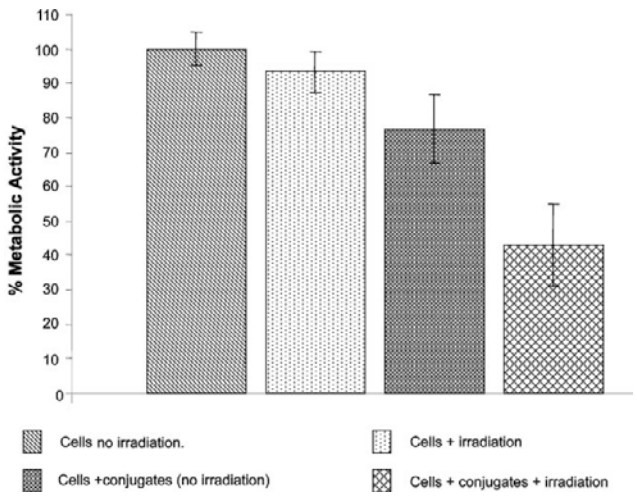

Fig. 5 Metabolic activity of HeLa cells, as determined by MTT assay, following incubation of phthalocyanine-nanoparticle conjugates (0.55 μM) for 4 h and subsequent irradiation at 690 nm (1.84 mW cm^{-2}) for 20 min.

When the internalised phthalocyanine-nanoparticle conjugates were irradiated at 690 nm, the HeLa cell viability decreased to 43% indicating that the majority of the cells had been killed through photodynamic action. The nanoparticle conjugates at the 0.55 μM concentration do appear to cause a partial 'dark' toxicity as the cell viability, without light irradiation, decreased to 77%. In order to establish whether a specific component of the conjugates was cytotoxic, each constituent was tested by measurement of cell viability. The components tested included TOAB and the free zinc phthalocyanine derivative both at concentrations determined to be present on the gold nanoparticle surface. The free phthalocyanine was solubilized using both TOAB and ethanol to facilitate incubation with the HeLa cells. To determine whether the gold was cytotoxic, mannose stabilized gold nanoparticles were produced and tested. The results of the 'dark' toxicity and the phototoxicity of each of these individual components are shown in Fig. 6.

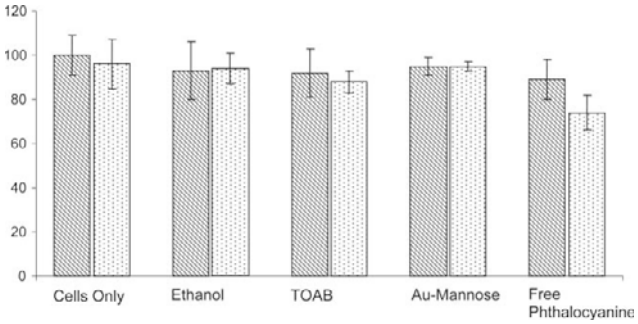

Fig. 6 HeLa cell viability (% metabolic activity), as determined by MTT assay, following incubation with the individual constituents of the phthalocyanine-nanoparticle conjugates: ethanol (0.5%); TOAB (2.19 μM); Au–mannose nanoparticles (0.42 μM); and zinc phthalocyanine derivative (0.55 μM, solubilized using TOAB and ethanol). Test solutions were each incubated with HeLa cells for 6 h in DMEM. Irradiation of samples was achieved using a 690 nm laser for 10 min at 1.84 mW cm^{-2}. Non-irradiated cells (diagonal shading), irradiated cells (dot shading). Results are an averaged value from 3 replicates.

Minimal cytotoxic effect was observed with the ethanol (cell viability of *ca.* 94%), and the mannose coated gold nanoparticles (95%) with or without red-light irradiation. Indeed, following the irradiation protocol a decrease in cell viability from 100 to 96% was induced in the cells alone. The incubation of the cells with the TOAB phase transfer reagent reduced the cell viability to 88% when the cells were irradiated. Addition of the free phthalocyanine derivative (solubilized with both TOAB and ethanol) to the cells also decreased the cell viability to 89%. A further decrease in cell viability was obtained (74%) when these cells were irradiated, showing the PDT effect of the phthalocyanine derivative. The 'dark' toxicity of the nanoparticle conjugates (Fig. 5) appears to represent a cumulative effect from the individual components.

From Fig. 5 it is apparent that a significantly enhanced photodynamic effect is observed with the phthalocyanine-nanoparticle conjugates with a decrease in cell viability to 43% as compared to the free phthalocyanine (Fig. 6). Indeed, these results show that the nanoparticle conjugates exhibit a PDT efficiency which is greater than twice that of the free phthalocyanine derivative. This is a substantial improvement in PDT efficiency which probably can be attributed to the 50% enhancement of singlet oxygen quantum yield observed for the phthalocyanine-nanoparticle conjugates as compared to the free photosensitizer.

Following PDT with the phthalocyanine-nanoparticle conjugates the morphology of the HeLa cells changes dramatically. The combined differential contrast and fluorescence microscopy images (Fig. 7(A)) shows the presence of the nanoparticle-conjugates within the intracellular environment of the HeLa cells but additionally the cells show the presence of blebs and vacuoles. These cellular features are not present in 'healthy' HeLa cells (Fig. 7(B)) and are indicative of cell mortality possibly induced by apoptosis.

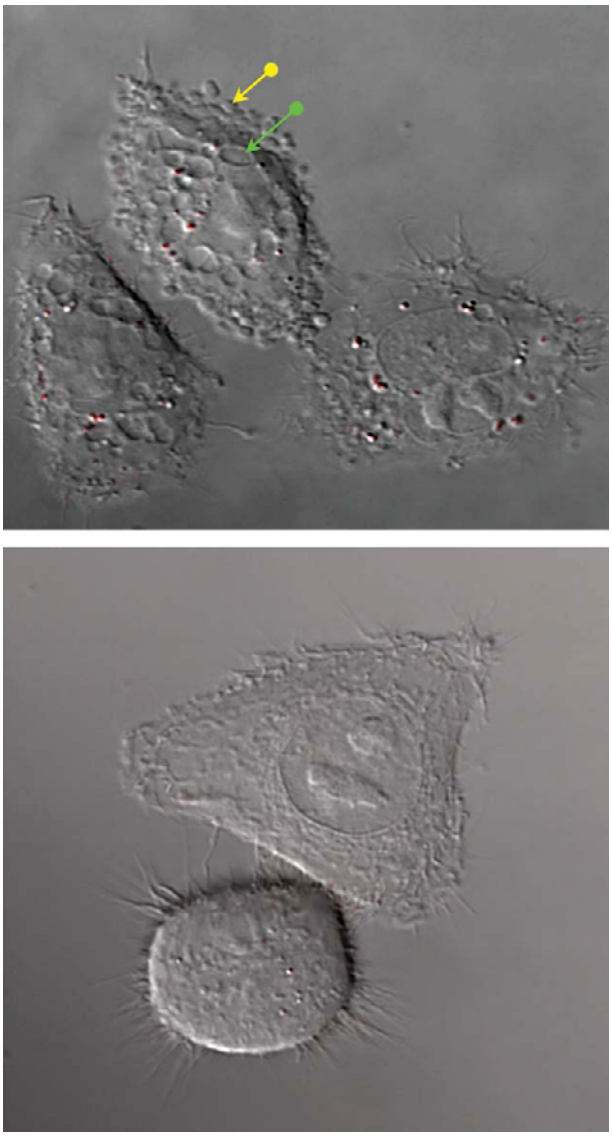

Fig. 7 Combined confocal fluorescence and DIC images of: (A) A post PDT image of phthalocyanine-nanoparticle conjugates internalised within HeLa cells following 6 h incubation and (B) 'Healthy' HeLa cells—with no nanoparticle conjugates. The cellular morphology in (A) shows the presence of blebs (yellow arrow) and vacuoles (green arrow), structures which are absent in the none PDT treated cells shown in (B).

To determine whether the nanoparticle conjugates induce apoptosis following PDT a caspase 3/7 assay was used. Caspase-3 is considered one of the central molecules in apoptotic events and is responsible for the cleavage and activation of caspase 6, 7 and 8.[23,24] The Caspase-Glo™ 3/7 assay measures the amount of caspase 3/7 by luminescence as the cleavage of caspase produces a luminescent signal from luciferase; the intensity of the luminescence signal being proportional to the quantity of caspase 3/7 produced. The average luminescence intensity (from 3 separate measurements) obtained from the caspase 3/7 assay following irradiation of the HeLa cells containing nanoparticle conjugates was 7875 RLU (relative light units), whereas the average intensity obtained for HeLa cells without the conjugates was 7333 RLU. The luminescence intensity obtained from the HeLa cells with non-irradiated nanoparticle conjugates was comparable to the cells without conjugates present. This latter result suggests that the non-irradiated nanoparticle conjugates do not induce apoptosis. However, the increased luminescence intensity following irradiation of the nanoparticle conjugates internalised by the HeLa cells indicates an enhanced level of caspase 3/7 suggesting that apoptosis is involved in the cellular death that is induced by PDT with the phthalocyanine-nanoparticle conjugates.

Both necrosis and apoptosis are known to be involved in cellular destruction through PDT.[23–25] The balance between these two mechanisms being dependent upon a range of parameters including light-dose, post-irradiation time, the concentration of photosensitizer, cell type, its genetic and metabolic potential, the nature of the photosensitizer and its sub-cellular localization.[23–25] Under the optimized experimental protocol conditions used to elicit cell kill with the nanoparticle conjugates, the luminescence caspase assay results suggest that apoptosis is intimately involved in the cell kill.

Conclusions

Gold nanoparticles stabilized with a hydrophobic phthalocyanine photosensitizer have been formulated with a typical diameter of 2–4 nm. The phthalocyanine, present as the monomeric species (*i.e.* non-aggregated) on the gold particle surface, absorbs light maximally at 695 nm. The phthalocyanine-nanoparticle conjugates, which are soluble in polar solvents, readily generate singlet oxygen following irradiation with a 690 nm diode laser. These properties suggest that the phthalocyanine-nanoparticle conjugates are ideally suited for PDT of cancer indications. Diluting the phthalocyanine-nanoparticle conjugates in buffer facilitates incubation with HeLa cells *in vitro*. The nanoparticle conjugates are taken-up by the HeLa cells, delivering the photosensitizer directly to the intracellular environment. Irradiation of the conjugates within the cells causes significant cell mortality through the photodynamic effect. Apoptosis is implicated as one mechanism by which PDT with the phthalocyanine-nanoparticle conjugates induces cell kill. While these results are extremely encouraging, the true test of the phthalocyanine-nanoparticle conjugates will come when their PDT efficacy is evaluated *in vivo*. The results of such studies will be presented in a future communication.

Acknowledgements

The assistance of Dr Nural Kabir with the confocal fluorescence microscopy images and Claire Schofield with the production of the figures is gratefully acknowledged. Financial support from the BBSRC (studentship for MEW) and the MRC/EPSRC (*Discipline hopping* award, G0100667, to DAR) is also gratefully acknowledged.

References

1 X. Guo, Y. Cui, R. M. Levenson, L. W. K. Chung and S. Nie, *In vivo* cancer targeting and imaging with semiconductor quantum dots, *Nat. Biotechnol.*, 2004, **22**, 969–976.
2 L. R. Hirsch, R. J. Stafford, J. A. Bankson, S. R. Sershen, B. Rivera, R. E. Price, J. D. Hazle, N. J. Halas and J. L. West, Nanoshell-mediated near-infrared thermal therapy of tumors under magnetic resonance guidance, *Proc. Natl. Acad. Sci. U. S. A.*, 2003, **100**, 13549–13554.

3 D. P. O'Neal, L. R. Hirsch, N. J. Halas, J. D. Payne and J. L. West, Photo-thermal tumor ablation in mice using near infrared-absorbing nanoparticles, *Cancer Lett.*, 2004, **209**, 171–176.
4 S. B. Brown, E. A. Brown and I. Walker, The present and future role of photodynamic therapy in cancer treatment, *Lancet Oncology*, 2004, **5**, 497–508.
5 M. J. Cook, I. Chambrier, S. J. Cracknell, D. A. Mayes and D. A. Russell, Octa-alkyl zinc phthalocyanines: Potential photosensitizers for use in the photodynamic therapy of cancer, *Photochem. Photobiol.*, 1995, **62**, 542–545.
6 T. J. Dougherty, C. J. Gomer, B. W. Henderson, G. Jori, D. Kessel, M. Korbelik, J. Moan and Q. Peng, Photodynamic therapy, *J. Nat. Cancer Inst.*, 1998, **90**, 889–905.
7 R. W. Boyle and D. Dolphin, Structure and biodistribution relationships of photodynamic sensitizers, *Photochem. Photobiol.*, 1996, **64**, 469–485.
8 C. Ometto, C. Fabris, C. Milanesi, G. Jori, M. J. Cook and D. A. Russell, Tumour-localising and -photosensitising properties of a novel zinc(II) octadecylphthalocyanine, *Br. J. Cancer*, 1996, **74**, 1891–1899.
9 C. Fabris, C. Ometto, C. Milanesi, G. Jori, M. J. Cook and D. A. Russell, Tumour-localizing and tumour-photosensitizing properties of zinc(II)-octapentyl-phthalocyanine, *J. Photochem. Photobiol., B*, 1997, **39**, 279–284.
10 D. C. Hone, P. I. Walker, R. Evans-Gowing, S. FitzGerald, A. Beeby, I. Chambrier, M. J. Cook and D. A. Russell, Generation of cytotoxic singlet oxygen *via* phthalocyanine-stabilized gold nanoparticles: A potential delivery vehicle for photodynamic therapy, *Langmuir*, 2002, **18**, 2985–2987.
11 I. Roy, T. Y. Ohulchanskyy, H. E. Pudavar, E. J. Bergey, A. R. Oseroff, J. Morgan, T. J. Dougherty and P. N. Prasad, Ceramic-based nanoparticles entrapping water-insoluble photosensitizing anticancer drugs: A novel drug-carrier system for photodynamic therapy, *J. Am. Chem. Soc.*, 2003, **125**, 7860–7865.
12 A. C. S. Samia, X. B. Chen and C. Burda, Semi-conductor quantum dots for photodynamic therapy, *J. Am. Chem. Soc.*, 2003, **125**, 15736–15737.
13 R. Bakalova, H. Ohba, Z. Zhelev, T. Nagase, R. Jose, M. Ishikawa and Y. Baba, Quantum dot anti-CD conjugates: Are they potential photosensitizers or potentiators of classical photosensitizing agents in photodynamic therapy of cancer?, *Nano Lett.*, 2004, **4**, 1567–1573.
14 S. M. J. Moreno, E. Monson, R. G. Reddy, A. Rehemtulla, B. D. Ross, M. Philbert, R. J. Schneider and R. Kopelman, Production of singlet oxygen by $Ru(dpp(SO_3)_2)_3$ incorporated in polyacrylamide PEBBLE, *Sens. Actuators, B*, 2003, **90**, 82–89.
15 F. Yan and R. Kopelman, The embedding of *meta*-tetra(hydroxyphenyl)-chlorin into silica nanoparticle platforms for photodynamic therapy and their singlet oxygen production and pH-dependent optical properties, *Photochem. Photobiol.*, 2003, **78**, 587–591.
16 H. Gu, K. Xu, Z. Yang, C. K. Chang and B. Xu, Synthesis and cellular uptake of porphyrin decorated iron oxide nanoparticles—a potential candidate for bimodal anticancer therapy, *Chem. Commun.*, 2005, 4270–4272.
17 S. Z. Wang, R. M. Gao, F. M. Zhou and M. Selke, Nanomaterials and singlet oxygen photosensitizers: Potential applications in photodynamic therapy, *J. Mater. Chem.*, 2004, **14**, 487–493.
18 J. Simard, C. Briggs, A. K. Boal and V. M. Rotello, Formation and pH-controlled assembly of amphiphilic gold nanoparticles, *Chem. Commun.*, 2000, 1943–1944.
19 K. K. Sandhu, C. M. McIntosh, J. M. Simard, S. W. Smith and V. M. Rotello, Gold nanoparticle-mediated transfection of mammalian cells, *Bioconjugate Chem.*, 2002, **13**, 3–6.
20 D. C. Hone, A. H. Haines and D. A. Russell, Rapid, quantitative colorimetric detection of a lectin using mannose-stabilised gold nanoparticles, *Langmuir*, 2003, **19**, 7141–7144.
21 B. A. Lindig, M. A. J. Rogers and A. P. Schaap, Determination of the lifetime of singlet oxygen in D_2O using 9,10-anthracene dipropionic acid, *J. Am. Chem. Soc.*, 1980, **102**, 5590–5593.
22 T. Mossman, Rapid colorimetric assay for cellular growth and survival: Application to proliferation and cytotoxicity assays, *J. Immunol. Methods*, 1983, **65**, 55–63.
23 D. J. Granville, C. M. Carthy, H. J. Jiang, G. C. Shore, B. M. McManus and D. W. C. Hunt, Rapid cytochrome c release, activation of caspases 3, 6, 7 and 8 followed by Bap31 cleavage in HeLa cells treated with photodynamic therapy, *FEBS Lett.*, 1998, **437**, 5–10.
24 L. Mooney, K. Al-Sakaaf, B. Brown and P. Dobson, Apoptotic mechanisms in T47D and MCF-7 human breast cancer, *Br. J. Cancer*, 2002, **87**, 909–917.
25 N. Oleinick, R. Morris and I. Belichenko, The role of apoptosis in response to photodynamic therapy: What, where, why and how?, *Photochem. Photobiol. Sci.*, 2002, **1**, 1–21.

